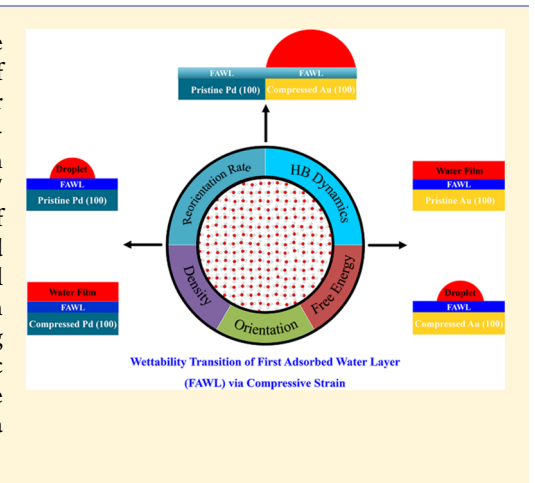
First Adsorbed Water Layer and Its Wettability Transition under **Compressive Lattice Strain**

Guobing Zhou,[†] Bradley H. Schoen,[†] Zhen Yang,[‡] and Liangliang Huang*,[†]

Supporting Information

ABSTRACT: A molecular-level description of a near-surface water structure and a handy manipulation of its properties are relevant to a broad range of scientific and technological phenomena. Here, through a series of molecular dynamics simulations, we report the observation and characterization of a lowmobility first adsorbed water layer (FAWL) and its tunable wetting transition at three metal surface models, namely, Au(100), Pd(100), and a Pd(100)/ Au(100) bimetallic junction. The results reveal that (i) there is a formation of the FAWL, resulting from competitive water-water hydrogen bonding and water-solid interactions, which in turn dictates the wettability at water-metal interfaces, (ii) applying compressive lattice strain to metal substrates can induce interfacial wettability transition, which is mediated by subtle packing changes of the FAWL, and (iii) by adjusting the lattice strains, the bimetallic junction can host a switchable wettability transition. We anticipate that those findings provide a rigorous fundamental understanding of how water wets a metal surface and how the wettability can be transited purposely.



1. INTRODUCTION

Downloaded via UNIV OF OKLAHOMA on January 7, 2021 at 01:07:00 (UTC). See https://pubs.acs.org/sharingguidelines for options on how to legitimately share published articles.

The water-metal interface is relevant to a broad range of scientific phenomena and technological processes in astrophysics, electrochemistry, and microelectromechanics, which include corrosion and heterogeneous catalysis, to name just a few. 1-5 When water molecules are in direct contact with a metal surface, forming the first adsorbed water layer (FAWL), a part of water-water hydrogen bonding interactions would be substituted by stronger water-solid interactions. From the microscopic point of view, the FAWL is a collection of water molecules whose physical and chemical properties are drastically altered by the metal surface.^{3,5} As a result of the interaction balance, various scenarios have been observed for the FAWL, including water decomposition, ice-like solid structure formation, and non-wetting behavior where water molecules from the FAWL are thermodynamically stabilized by a combination of in-plane water-water and out-plane watermetal interactions.³⁻⁵ In return, the FAWL effectively serves as a one-molecule thin boundary between liquid water and a solid metal, mediating the liquid properties at those surfaces. There is a pressing need to understand the structure and dynamic properties of the FAWL and comprehend their relevance to and impact on the processes occurring at water-metal interfaces.

Delicately modulating and modifying the wettability of solid surfaces have triggered tremendous research interest in the last decade.6-16 Prior studies have demonstrated that the wettability of solid surfaces is directly dominated by the

formed FAWL. 13-19 Low temperature experiments revealed specific in-plane interactions of water molecules of the FAWL dominate the wetting properties of the Pt(111) surface. 19 Molecular dynamics (MD) simulations revealed the same phenomenon for Pt(100) and (111) surfaces at room temperature, where the degree of hydrophobicity of the FAWL was attributed to its passivated hydrogen bond (HB) network.¹⁸ Generally speaking, the properties of the FAWL are tunable via balancing the HB interactions within the water monolayer and water-surface interactions, 3,5 both of which depending significantly on intrinsic chemistry and the structural properties of solid surfaces. 3,5,13,14

Substantial strategies have been proposed to alter interactions at the water-solid interface, which in turn allow the manipulation of interfacial wettability. 7-18,20-26 Successful demonstrations include coating hydrophobic graphene to reduce water-surface interactions²⁰ and chemically adding surface terminal groups (-CH₃, -CF₃, -OH, -COOH, etc.)^{21–24} to intentionally weaken or strengthen water–surface interactions. Promising progress has also been achieved from structural manipulations, by the engineering of roughness, $^{7-10,12,21}$ curvature, 14 or morphology 13,15,17,18 of solid surfaces. This work presents an alternative manipulation via applying compressive lattice strains to metal surfaces.

Received: July 17, 2019 Revised: November 12, 2019 Published: November 18, 2019

[†]School of Chemical, Biological and Materials Engineering, University of Oklahoma, Norman, Oklahoma 73019, United States ‡Institute of Advanced Materials (IAM), State-Province Joint Engineering Laboratory of Zeolite Membrane Materials, College of Chemistry and Chemical Engineering, Jiangxi Normal University, Nanchang 330022, People's Republic of China

Malleability, weldability, and generally large Young's modulus enable the use of metals and metal junctions under external harsh stresses, while maintaining the integrity and reversibility of the metal properties. Various studies ^{13,27,28} indicated that lattice strain can affect water—surface interactions, but such knowledge is far from mature.

By a series of MD simulations, we explore the effect of compressive lattice strain on the FAWL formation and its wettability. Three metal surface models have been constructed and investigated, namely, the monometallic Au(100), Pd(100) surfaces, and the Pd(100)/Au(100) bimetallic junction. It is worth noting that lattice constants of Au and Pd are 4.08 and 3.89 Å, respectively. For the (100) facet, the atomic distances of Au-Au (2.88 Å) and Pd-Pd (2.75 Å) are close to that of water-water (2.77 Å) of an hexagonal close packed ice structure, potentially favoring water adsorption at atop Au (or Pd) sites and assisting the formation of a low-mobility FAWL. For the Pd(100)/Au(100) bimetallic junction, the Au(100) surface with a larger lattice constant was compressed in the y direction to match the lattice of the Pd(100) surface. In particular, special attention has been paid to the structural and dynamical properties, including the density and orientation distribution, HB dynamics, reorientation rate, and free energy profile, of the FAWL on the bimetallic Pd(100)/Au(100) junction system. By comparison, we reported that the FAWL on the pristine Pd(100) region is much more stable compared with that on the compressed Au(100) region, thereby demonstrating its hydrophobic nature and property of repelling bulk water from pristine Pd(100) to compressed Au(100).

2. MODELS AND SIMULATION DETAILS

2.1. Surface Models. Pristine Pd(100) and Au(100) surfaces and a Pd(100)/Au(100) bimetallic junction model have been constructed to investigate the properties of the FAWL. For compressed pristine surfaces, the strain was applied biaxially along X and Y directions, varying from 0 to 5%. Strain δ is defined as $\frac{a_0-a}{a_0}$, where a_0 and a are, respectively, the pristine equilibrium lattice constant and lattice under a compressive strain. The strain is applied by linearly rescaling the x and y coordinates of all the atoms of the substrate by a factor of $(1-\delta)$, as shown in Figure 1. Other

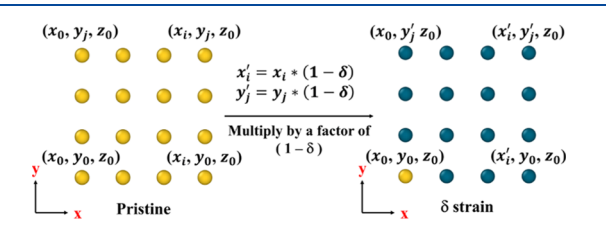


Figure 1. A schematic illustration of the compressive strain applied in the simulations.

simulation details are available in Table S1 of the Supporting Information. The bimetallic junction consisted of a pristine Pd(100) and a compressed Au(100). A monoaxial strain of 4.61% was applied along the Y direction to Au(100), so that the compressed lattice constant matched that of the pristine Pd(100). The surfaces were kept rigid during all MD calculations. Metal sites were regarded as uncharged and only van der Waals (vdW) interactions were considered between water and the metal. Nonbonded vdW parameters of

Pd and Au were derived from the force field developed by Heinz et al.,²⁹ which has been widely adopted to probe the metal interfacial properties and metal interactions with water and biomolecules. 14,17,30-32 Although the applied force field did not consider the polarization effect, prior studies have demonstrated that the employed force field could qualitatively reproduce both the structure and the interaction energy profile of water on face-centered cubic metal surfaces. 14,177, flexible extended simple point charge (SPCE-F) model³³ was used for water, in which the O-H bond and the H-O-H angle are described by harmonic potentials, with the bond constant, $k_{\rm b}$, 1108.57 kcal/(mol·Å²) and the angle constant, $k_{\rm th}$ 91.54 kcal/(mol·rad²). Toukan and Rahman³⁴ demonstrated that a flexible SPC water model can provide a good description of the water dynamic properties. Furthermore, Yuet and Blankschtein³³ pointed out that the flexibility of the O-H bond plays a key role in the surface tension of water at the interface. Their MD simulation study with the flexible SPC/E water model reported a surface tension of 70.2 mN/m, which agrees well with the experimental value of 71.7 mN/m.³³ For the wettability studies of liquid water, the dynamic diffusion and surface tension are two critical parameters that influence the wetting behavior of water on solid surfaces. Therefore, the flexible SPC/E water model was employed in this work. For the simulation box, the metal surface was fully covered by a water film with a thickness of 1.0 nm. For the choice of the initial water geometry, prior studies 16,17 reported that when the water film was employed to explore the wettability of solid substrates, a cylindrical nanodroplet was formed above the FAWL. Bratko and coworkers demonstrated that the calculated contact angle from the cylindrical water droplet can minimize the deviation from what is predicted by Young's equation. An extra vacuum of 5.0 nm was added above the water film in the Z direction to avoid the interactions between periodic images. More details are shown in Figures S1-S3 and Table S1 of the Supporting Information. Periodic boundary conditions were applied in all three directions. The Lennard-Jones (LJ) 12-6 potential was utilized to describe waterwater and water-metal vdW interactions. In addition, waterwater electrostatic interactions were described by Coulomb's law. The LJ parameters and atomic charges used in this study are available in Table S2. The L-J parameters for unlike pairs are obtained using the Lorenz-Berthelot mixing rules, that is, the arithmetic mean (Lorentz's) for size parameters, and the geometric mean (Berthelot's) for energy parameters. While Heinz and co-workers²⁹ used Berthelot's rule for both size and energy parameters, our test calculations show that the choice of the mixing rule does not change the observed phenomena.

2.2. Simulation Details. All MD simulations were carried out with the *NVT* ensemble using the LAMMPS software package.³⁶ The Nose–Hoover thermostat was used to maintain the temperature of a simulation system at 300.0 K with a coupling coefficient of 0.1 ps. Initial velocities of water molecules were assigned according to the Boltzmann distribution. Newton's equation was integrated by the velocity Verlet algorithm with a time step of 1.0 fs. The cutoff for nonbonded interactions was set to be 1.0 nm, with a skin distance of 0.2 nm to store the pairwise neighboring list, which was updated every 10 steps. The long-range electrostatic interactions were calculated by the particle—particle particle—mesh algorithm with an accuracy of 10^{-5} .³⁷ For each system, a calculation of 30.0 ns was carried out, where the first 15.0 ns was for equilibrium, and the latter 15.0 ns was for data analysis,

in which the trajectory was stored every 100.0 fs. After the 30.0 ns simulation, a successive NVT simulation was performed for HB dynamic property calculations, in which the simulation was performed for 500 ps with the trajectory being updated every 5 fs.

3. RESULTS AND DISCUSSION

3.1. Pristine Monometallic Pd(100) and Au(100) Surfaces. Figure 2 shows the equilibrium structures of water

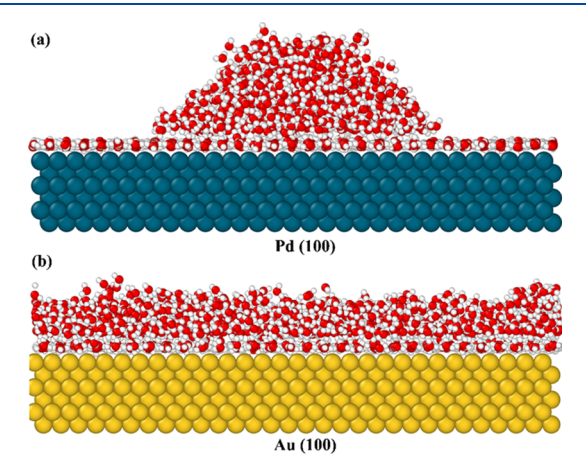


Figure 2. The equilibrium configuration of a 1.0 nm water film on (a) Pd(100); (b) Au(100). An ordered FAWL was observed on both surfaces but with significantly different wettability properties: hydrophobic for Pd(100); hydrophilic for Au(100).

on pristine metal surfaces. Both Pd(100) and Au(100) host a layer of adsorbed water of one-molecule thickness. For Pd(100), the FAWL formed is hydrophobic in nature, stabilizing a water droplet, and such a unique feature is independent of the water model (see Figure S4) and the initial water geometry (see Figure S5). In contrast, the FAWL of Au(100) is hydrophilic, witnessed by a fully wetting water film.

It should be noted that the FAWL is consisted of those water molecules within a distance of 4 Å from the metal surface, which corresponds to the first solvation shell in the density distribution profiles, see Figure S6 of the Supporting Information. Such ordered FAWL-induced hydrophobicity was observed previously. 16-19 From the perspective of intermolecular interactions, the FAWL results from the competitive yet subtle Gibbs free energy balance between water-water hydrogen bonding and water-metal interactions. The water-metal interactions preferentially substitute waterwater interactions of the bulk, gradually changing the interaction strength between the FAWL and surrounding bulk water, and eventually leading to the phenomenon that other water molecules above the FAWL accumulate to form a water droplet, as that revealed at the FAWL of Pd(100). It is worth noting that the size of a water droplet at the Pd(100) surface is dominated by the interaction difference between water-water and water-metal, as well as the thickness of the initial water film, see the detailed discussion in Section 6 of the Supporting Information S6.

3.2. Monometallic Pd(100) and Au(100) Surfaces under Compressive Lattice Strain. Under operational conditions, devices are exposed to various stresses, thereby yielding different elastic strains. To probe the lattice strain effect on the formation of the FAWL and its wettability properties, five compressive strains were applied to Pd(100) and Au(100) surfaces, biaxially along the X and Y directions. The strains studied in this work are up to 5%, corresponding to external loads of about 0.3 GPa for Au³⁸ and 5 GPa for Pd, 35 which are interpolated from their mechanical property diagrams. Results in Figure 3 reveal an interesting wettability transition due to the applied compressive strain. For comparison, the pristine Pd(100) and Au(100) surfaces are also shown. First of all, the FAWL was observed for both metals under studied strains. When the strain was within 4% for the Pd(100) surface, there existed a stable water droplet on the FAWL. However, when the strain was increased to 5%, a

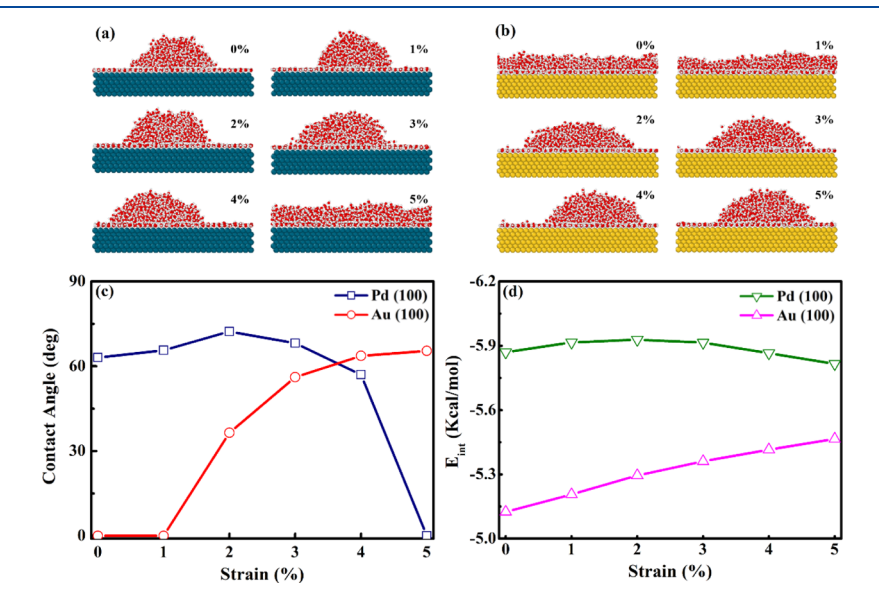


Figure 3. Equilibrium configurations of a 1.0 nm water film on metal surfaces under compressive strains: (a) Pd(100); (b) Au(100). 0% strain represents a pristine metal surface. Strains up to 5% have been studied, corresponding to \sim 0.3 GPa for Au and \sim 5.0 GPa for Pd, respectively; (c) calculated contact angles of water droplets at Pd(100) and Au(100) surfaces; (d) interaction energies between the FAWL and the metal surfaces. All standard deviations are less than \pm 2.73°. A list of values is shown in Table S3 of the Supporting Information.

hydrophobic to hydrophilic wettability transition occurred. As demonstrated in Figure 3a, a complete wetting water film was observed on the FAWL. Phan et al. 40 also reported resembled wetting transition from hydrophobic to hydrophilic for the water droplet on the MgO surface by controlling the vibration of surface atoms. In addition, a similar wettability transition, hydrophilic to hydrophobic, was also observed for the Au(100) surface under compressive strains. For the cases with strains from 2 to 5%, the FAWL of the Au(100) surface respells bulk water, generating and stabilizing the formed water droplet. Furthermore, our simulation results also demonstrated that the generated water droplet is not sensitive to the surface flexibility, see Figures S13—S15.

To quantitatively describe the wettability transition, we analyzed the contact angle of water droplets. The calculation details are available in Section 8 of the Supporting Information S8. Similar to the work of Zhu and co-workers, 14 we defined the contact angle to be 0° when the water droplet disappears from a hydrophilic FAWL. As shown in Figure 3c, when the strain is less than 4%, contact angles of water droplets of the Pd(100) surface are 63.09 ± 1.43 , 65.67 ± 2.01 , 72.30 ± 1.31 , 68.20 ± 2.73 , and $57.03 \pm 1.93^{\circ}$, corresponding to strains of 0, 1, 2, 3, and 4%, respectively. When it comes to the Au(100) surface, the contact angle increases from 0 to 65.0° (see the list of values in Table S3 of the Supporting Information) with the change of compressive strains from 0 to 5%, indicative of a hydrophilic to hydrophobic wettability transition. Upon further increasing the strain to 6% for the Au(100) surface (see Figure S17), the contact angle is calculated to be $69.24 \pm 0.66^{\circ}$, which is slightly larger than that of the 5% strain case, $65.45 \pm 1.32^{\circ}$. In addition, the interaction energy between the FAWL and the metal surface was also calculated, see details in Section 10 of the Supporting Information S10. From Figures 3d and S20 and Table S4 of the Supporting Information, when the formed FAWL demonstrates distinct hydrophobic nature, there is a significant increase of both the interaction energy between the FAWL and the metal surface, and the HB strength within the FAWL. The enhanced interaction energy would result in stronger binding strength between the FAWL and the metal surface. Meanwhile, the increased HB strength indicates that water molecules in the FAWL prefer to form HBs within the monolayer, rather than with other water molecules above the FAWL. By combining the contributions from the two parts, we conclude that the stability of the FAWL is largely determined by the interaction energy between the FAWL and metal surfaces. The HB interactions within the monolayer can in turn tune the wetting properties of the FAWL. Therefore, a hydrophobic FAWL generally demonstrates a better stability. In other words, water molecules from a more hydrophobic FAWL interact much weakly with water molecules above the FAWL. This trend is also confirmed by the orientational analysis and HB distribution of the FAWL, as discussed in the Supporting Information.

On the other hand, Wang and co-workers¹⁷ pointed out that the lattice constant of the solid substrate also has a significant influence on the properties of the FAWL. Therefore, we have estimated the average distance of the adjacent oxygen—oxygen (O—O) in the FAWL. The results in Table 1 show that, for the hydrophobic FAWL on both Pd(100) and Au(100) surfaces, there is a good match between the lattice constant and the average O—O distance of the FAWL, which favors the increase of the average HB number within the FAWL and a more stable HB network, in quite agreement with the HB results shown in

Table 1. Lattice Constant and Water–Water Distance in the FAWL on the Metal Surfaces with Various Strains^a

Substrate	Strain	Lattice Constant	Water-Water	Relative Difference
	Suam	(Å)	Distance (Å)	(Å)
Pd (100)	0%	2.750	2.754±0.002	0.004
	1%	2.723	2.739±0.002	0.016
	2%	2.695	2.724±0.002	0.029
	3%	2.668	2.718±0.002	0.050
	4%	2.640	2.718±0.003	0.078
	5%	2.613	2.743±0.004	0.130
Au (100)	0%	2.880	2.773±0.003	0.107
	1%	2.851	2.773±0.003	0.077
	2%	2.822	2.776±0.003	0.046
	3%	2.794	2.769 ± 0.002	0.025
	4%	2.765	2.759±0.002	0.006
	5%	2.736	2.748±0.002	0.012

⁴Note: the green and yellow refer to the FAWL with hydrophobic and hydrophilic features, respectively.

Figures S19 and S20 of Supporting Information. In contrast, for the hydrophilic FAWL on both Pd(100) and Au(100) surfaces, the structure of the FAWL would be much more easily disturbed by water molecules present above the FAWL, due to the mismatch between the O–O distance and the lattice constant, and therefore it is difficult for them to form a droplet on the FAWL. Such results enable us to conclude that a good match between the lattice constant of a substrate and the adjacent O–O distance of a FAWL would benefit the FAWL to show a feature of hydrophobicity.

3.3. Bimetallic Junction of Pd(100)/Au(100). The compressive strain induced wettability transition, in particular, the reverse correlation with respect to Pd(100) and Au(100) surfaces, triggered another fundamental discussion: for a bimetallic junction where the metal with a larger lattice constant is usually compressed to match the lattice of the other metal, what would be the FAWL and its wettability property? To shed light on this question, we constructed a bimetallic junction model consisting of Pd(100) and Au(100) surfaces and studied the wetting behavior of a thin water film on this bimetallic junction. As illustrated in Figure 4, a compressive strain of 4.61% was applied to the Au(100) surface monoaxially along the Y direction to match lattice constants. No strain was applied to the Pd(100) surface. Similar to the aforementioned discussions, an initial thin water film of 1.0 nm was then placed on the bimetallic surface (see Figure 4a). As expected, an ordered FAWL was formed on the bimetallic junction after reaching equilibrium, as shown in Figure 4b. More interestingly, a water droplet was observed from the compressed Au(100) region, and there was almost no water molecule left atop of the FAWL of the pristine Pd(100). Multiple independent calculations have been carried out, all returning to the same equilibrium configuration of Figure 4b with an averaged contact angle of $62.27 \pm 0.81^{\circ}$ to the water droplet. It is worth noting that the water droplet is determined by the thickness of the initial water film, that is, the total number of water molecules. When the initial water film was reduced to 0.5 nm, a smaller water droplet was observed. However, for a thicker 1.5 nm initial water film, no water droplet but full wetting was observed. A more detailed discussion is available in the Supporting Information, see Figures S7-S8. Our simulation results revealed that, when the The Journal of Physical Chemistry C

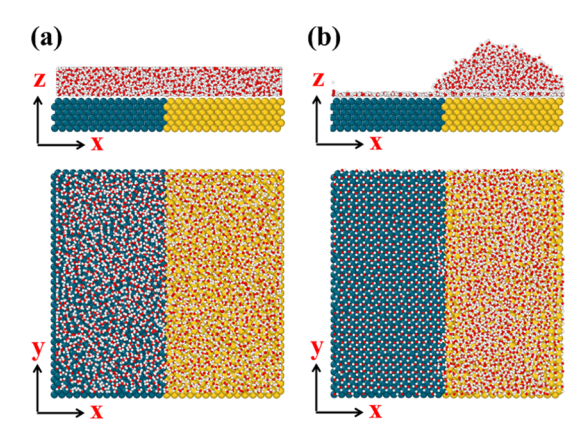


Figure 4. Schematic illustration of the simulation system of a bimetallic junction model. First, two separate metal surfaces, Pd(100) and Au(100), were prepared and then the Au(100) surface is uniformly compressed in the Y direction (4.61% strain) to match the lattice constant of Pd(100). A water film of 1.0 nm was placed on the obtained bimetallic junction. Side and top views of (a) the initial simulation box; (b) the simulation box at equilibrium where a water droplet is on the top of the compressive Au(100) region.

system is at a higher temperature of 350 K, the calculated contact angle for the water droplet is $54.60 \pm 0.86^{\circ}$ (Figure S23), smaller than that of the 300 K case, $62.27 \pm 0.81^{\circ}$, which means the shape of the water droplet is influenced by the temperature.

It has been reported that the properties of the FAWL directly dominate the behavior of water molecules on top. ^{13–19,24,28} According to the results shown in Figure 3, both the pristine Pd(100) and the 4.61% strain compressed Au(100) could host a hydrophobic FAWL with a water droplet. Therefore, the observed phenomenon of Figure 4 shall originate from the two FAWLs of Pd and Au regions. Detailed

analyses have been performed to probe their property difference. First, as presented in Figure 5a, the distribution of water molecules of the FAWL was revealed by the lateral density characteristics. The location of each water was labeled by the oxygen, Ow. The position of the pronounced first peak, 2.73 Å for Pd(100) and 2.71 Å for Au(100), denotes the distance between the nearest neighboring water molecules in the FAWL. Since the density at the first peak correlates with the packing order, it is obvious that the FAWL of pristine Pd(100) is more ordered than that of compressed Au(100). As discussed in Figure 3d, this is primarily ascribed to the interaction between the FAWL and the metal substrate. The FAWL of pristine Pd(100) has a stronger interaction with the metal substrate, -5.909 ± 0.006 kcal/mol. For compressed Au(100), it is -5.412 ± 0.004 kcal/mol.

Other static properties also support the conclusion that the pristine Pd(100) has a more stable and a more hydrophobic FAWL. Figure 5b,c are, respectively, the distribution probabilities of the dipole moment and the O-H bond of water molecules in the FAWL. As illustrated in the insets, the orientation of water is characterized by angles θ and φ : θ is defined as the angle between the dipole moment projection in the XY plane and the unit vector along the X direction; φ is the angle formed by the O-H bond and the unit vector normal to the metal substrate. For the dipole moment, four characteristic peaks were identified for both Pd and Au, namely, the ones at 45, 135, 225, and 315°. The unanimously larger probabilities (i.e., higher peaks) reveal a more ordered FAWL of pristine Pd(100) than the counterpart of compressed Au(100). For the O-H bond distribution of the FAWL, three potential orientations have been proposed: (a) O-H bonds point towards bulk water on top (B type); (b) O-H bonds are parallel to the substrate surface (P type); (c) O-H bonds point to the substrate surface (S type). For the pristine

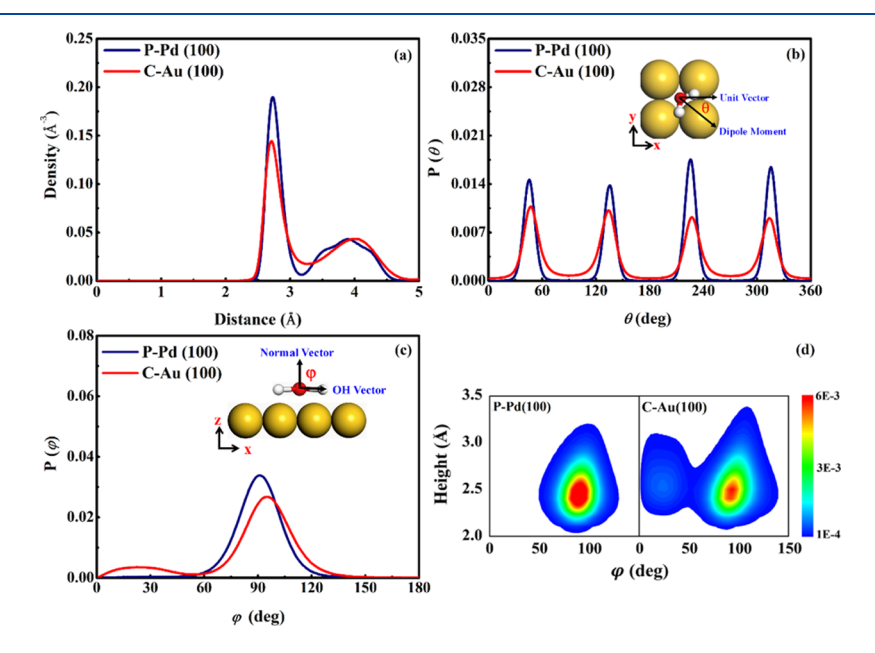


Figure 5. (a) Lateral density distribution of Ow–Ow for water molecules of the FAWL from both the pristine Pd(100) and compressed Au(100) regions; (b) probability of the dipole distribution angle θ , which is defined as the angle between the projection of the dipole moment in the x-y plane and the unit vector along the x direction; (c) probability of the O–H bond distribution angle φ , formed by the O–H bond and the unit vector normal to the metal substrate; (d) orientation distribution of water in the FAWL as a function of height h above the substrate and angle formed by the O–H bond and the surface normal vector. Note: the insets of (b,c) show schematic illustrations of θ and φ angles. Note: P–Pd (100) and C–Au (100) refer to the pristine Pd(100) and compressed Au(100) surfaces, respectively.

Pd(100), water molecules in the FAWL are of the P type, ~90°, suggesting that O-H bonds are uniformly parallel to the Pd substrate. Whereas on the compressed Au(100) surface, two representative O-H bond distributions were identified, one major peak at around 95° and one minor peak at around 25°, which correspond to P type O-H bonds parallel to the Au substrate and B type O-H bonds pointing towards bulk water on top, respectively. Those P type O-H bonds form a hydrogen bonding network with in-plane neighboring water molecules. The B type O-H bonds suggest that there exists a HB network between the FAWL and the atop bulk water. A detailed HB analysis shows that for the pristine Pd(100), the average number of in-plane HB (FAWL-FAWL) is 3.69, while the number of out-plane HB (FAWL-bulk water atop) is zero. For the compressed Au(100), the values are 3.06 and 0.51, respectively. The correlation of height and the O-H bond orientation of water of the FAWL in Figure 5d further supports the conclusion that water molecules in the FAWL of pristine Pd(100) interact exclusively with the Pd substrate and among themselves. In contrast, for the compressed Au(100), a significant amount of water molecules of the FAWL also interact with water from the bulk.

The analyses so far have revealed that the formation, the preferential water-metal adsorption sites, and the wettability difference are due to the subtle structural difference between the FAWL at pristine Pd(100) and compressed Au(100). How water of the FAWL behaves dynamically at interfaces is also highly valuable. Using the continuous time correlation functions (TCFs), the HB dynamic property, $S_{HB}(t)$, was calculated and presented in Figure 6a. As the result shows, for the FAWL of pristine Pd(100), the $S_{HB}(t)$ curve decays evidently slower than that of the compressed Au(100). This suggests a more stable HB network on the pristine Pd(100). Meng and coworkers proposed that the dynamic stability of the FAWL could be characterized by the reorientation rate, 13 which is derived from the second order Legendre polynomial time correlation function, $C_2(t)$. More discussions are available in Section 14 of the Supporting Information S14. Figure 6b displays the rate of water reorientation of the FAWL on pristine Pd(100) and compressed Au(100). It is prominent that water reorientation decays distinctly slower for the FAWL of the pristine Pd(100) region. Thus, both HB dynamics and the water reorientation rate conclude that the FAWL of the pristine Pd(100) region is much more stable, demonstrating hydrophobicity and the property of repelling other bulk water from the pristine Pd(100) to compressed Au(100) region.

Another descriptor of the dynamic stability is the self-diffusion coefficient, which is measured by calculating the mean squared displacement (MSD). As depicted in Figure S24, the MSD profiles of water molecules on both pristine Pd(100) and compressed Au(100) surfaces increase with respect to the simulation time, particularly for the latter one, indicative of an obvious diffusion feature of the liquid state. In addition, as shown in Table S5, the diffusion coefficients of water molecules on pristine Pd(100) and compressed Au(100) surfaces are two and 1 order of magnitude lower than those of bulk water, respectively. Those results reveal that the self-diffusion of the FAWL is generally very slow. To elucidate the dynamic property difference of the two FAWLs, the free energy profile of water molecules in the FAWL has been calculated according to the following equation⁴¹

$$\Delta G(x, y) = -k_{\rm B}T \ln P(x, y)$$

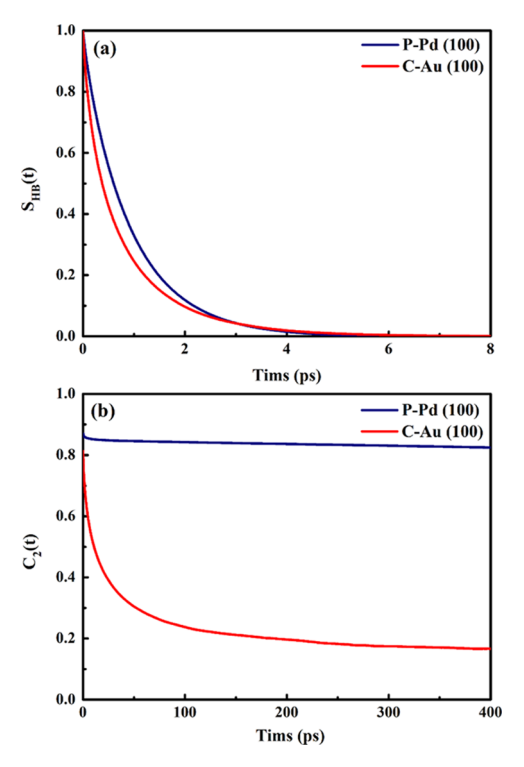


Figure 6. (a) Continuous time correlation functions, $S_{\rm HB}(t)$, for the HB network formed within the FAWL on pristine Pd(100) and compressed Au(100) surfaces; (b) the second-order reorientational TCF $C_2(t)$ for water molecules in the FAWL of pristine Pd(100) and compressed Au(100). Note: the P–Pd (100) and C–Au (100) refer to the pristine Pd(100) and compressed Au(100) surfaces, respectively.

where P(x,y) is the two-dimensional spatial probability distribution function of the oxygen atom of a water molecule in the FAWL, with its coordinate (x, y) projected to the metal plane; $k_{\rm B}$ is Boltzmann's constant; T is the temperature, in this work, 300 K; $\Delta G(x,y)$ is the projected free energy profile, a smaller value representing a stronger interaction and a better stability. This free energy calculation (see details in Section 16 of the Supporting Information S16) has been successfully employed for the slippage of water molecules on solid surfaces and the free energy profile of protein folding. $^{28,41-43}$

The free energy profile of Figure 7 clearly shows that the free energy profile of the FAWL of pristine Pd(100) is much more corrugated than that of the compressed Au(100) region. The free energy difference of the pristine Pd(100) region reaches 20.22 kJ/mol, while that of the compressed Au(100) is only about 12.72 kJ/mol. That corresponds to a nearly 60% decrease in the free energy profile to the FAWL of the compressed Au(100) region, leading to a much smaller energy barrier to water mobility. To conclude, the FAWL of the pristine Pd(100) region has a larger energy barrier for diffusion, and a higher dynamic stability, which in return favors the departure of bulk water atop, and results in the phenomenon shown in Figure 4: water accumulates on top of the compressed Au(100) region while no water stays atop of the FAWL of the pristine Pd(100).

4. CONCLUSION

A rigorous molecular-level description of water at interfaces continues to be a pressing need to nanoscience and advanced manufacturing. This work reports computational studies to

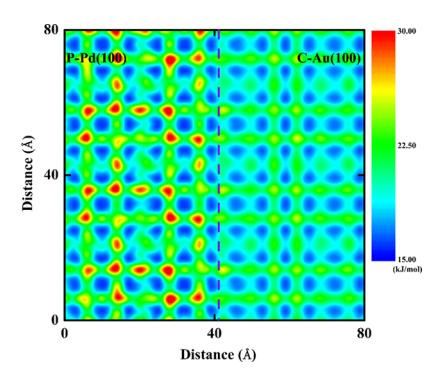


Figure 7. Free energy profile of water molecules in the FAWL of pristine Pd(100) and compressed Au(100) regions. The dashed line indicates the boundary of the two regions. Note: P-Pd(100) and C-Au(100) refer to the pristine Pd(100) and compressed Au(100) surfaces, respectively.

understand the behavior of the FAWL on metal surface models, namely, Au(100), Pd(100), and a Pd(100)/Au(100) bimetallic junction. The structural and dynamic properties of the FAWL have been discussed in detail. In addition, by applying compressive strains, we reveal a handy manipulation of the wettability properties of the FAWL: for a pristine metal surface, applying compressive strain can induce a transition of the interfacial wettability, which is mediated by subtle packing changes of the FAWL; for a bimetallic junction, the wettability is more complex, which is balanced by competitive waterwater and water-metal interactions. Considering the technology relevance and the known formation descriptor to the FAWL at interfaces, our study elucidates an exciting fundamental understanding to the next level: why a lowmobility water structure repels liquid water and how interfacial wettability could be purposely transited. Since the mobility of water molecules on the surface is closely related to the temperature, it would be quite interesting and important to explore the temperature effect on the wetting properties of the FAWL in the near future.

ASSOCIATED CONTENT

S Supporting Information

The Supporting Information is available free of charge at https://pubs.acs.org/doi/10.1021/acs.jpcc.9b06815.

Initial configurations of the simulation systems; simulation model details; LJ parameters and atomistic charges used in this work; water model and initial water geometry discussion; vertical density distribution of water molecules; water film thickness discussion; surface flexibility discussion; contact angle calculation; extra strain investigation; interaction energy calculation; HB definition and analysis; orientation analysis; temperature effect discussion; reorientation rate calculation; mean square displacement analysis; free energy profile calculations; and structural order parameter analysis (PDF)

AUTHOR INFORMATION

Corresponding Author

*E-mail: hll@ou.edu.

ORCID ®

Zhen Yang: 0000-0002-5205-3281 Liangliang Huang: 0000-0003-2358-9375

Author Contributions

G.Z. and L.H. designed the research and developed the model. G.Z. and B.S. performed the simulations and collected the data. G.Z., Z.Y., and L.H. analyzed and interpreted the data. All authors contributed to writing the paper.

Notes

The authors declare no competing financial interest.

ACKNOWLEDGMENTS

G.Z. and L.H. acknowledge the U.S. National Science Foundation (NSF) for support through grant CHE-1710102. L.H. also acknowledges the startup support from the University of Oklahoma. Z.Y. acknowledges the support by the National Natural Science Foundation of China (no. 21873046). We are very pleased to thank the OU Supercomputing Center for Education & Research (OSCER) at the University of Oklahoma for their dedicated support.

REFERENCES

- (1) Maier, S.; Salmeron, M. How Does Water Wet a Surface? *Acc. Chem. Res.* **2015**, 48, 2783–2790.
- (2) Hodgson, A.; Haq, S. Water Adsorption and the Wetting of Metal Surfaces. Surf. Sci. Rep. 2009, 64, 381–451.
- (3) Carrasco, J.; Hodgson, A.; Michaelides, A. A Molecular Perspective of Water at Metal Interfaces. *Nat. Mater.* **2012**, *11*, 667–674.
- (4) Shimizu, T. K.; Maier, S.; Verdaguer, A.; Velasco-Velez, J.-J.; Salmeron, M. Water at Surfaces and Interfaces: From Molecules to Ice and Bulk Liquid. *Prog. Surf. Sci.* **2018**, *93*, 87–107.
- (5) Björneholm, O.; Hansen, M. H.; Hodgson, A.; Liu, L.-M.; Limmer, D. T.; Michaelides, A.; Pedevilla, P.; Rossmeisl, J.; Shen, H.; Tocci, G.; Tyrode, E.; Walz, M.-M.; Werner, J.; Bluhm, H. Water at Interfaces. *Chem. Rev.* **2016**, *116*, 7698–7726.
- (6) Tian, Y.; Su, B.; Jiang, L. Interfacial Material System Exhibiting Superwettability. *Adv. Mater.* **2014**, *26*, 6872–6897.
- (7) Liu, K.; Jiang, L. Metallic Surfaces with Special Wettability. *Nanoscale* **2011**, *3*, 825–838.
- (8) Yao, X.; Song, Y.; Jiang, L. Applications of Bio-inspired Special Wettable Surfaces. *Adv. Mater.* **2011**, 23, 719–734.
- (9) Zhang, S.; Huang, J.; Chen, Z.; Lai, Y. Bioinspired Special Wettability Surfaces: From Fundamental Research to Water Harvesting Applications. *Small* **2017**, *13*, 1602992.
- (10) Wang, Z.; Elimelech, M.; Lin, S. Environmental Applications of Interfacial Materials with Special Wettability. *Environ. Sci. Technol.* **2016**, *50*, 2132–2150.
- (11) Su, B.; Tian, Y.; Jiang, L. Bioinspired Interfaces with Superwettability: From Materials to Chemistry. *J. Am. Chem. Soc.* **2016**, 138, 1727–1748.
- (12) Xin, B.; Hao, J. Reversibly Switchable Wettability. *Chem. Soc. Rev.* **2010**, *39*, 769–782.
- (13) Zhu, C.; Li, H.; Huang, Y.; Zeng, X. C.; Meng, S. Microscopic Insight into Surface Wetting: Relations between Interfacial Water Structure and the Underlying Lattice Constant. *Phys. Rev. Lett.* **2013**, *110*, 126101.
- (14) Zhu, Z.; Guo, H.; Jiang, X.; Chen, Y.; Song, B.; Zhu, Y.; Zhuang, S. Reversible Hydrophobicity-Hydrophilicity Transition Modulated by Surface Curvature. *J. Phys. Chem. Lett.* **2018**, *9*, 2346–2352.
- (15) van der Niet, M. J.; den Dunnen, A.; Koper, M. T.; Juurlink, L. B. Tuning Hydrophobicity of Platinum by Mmall Changes in Surface Morphology. *Phys. Rev. Lett.* **2011**, *107*, 146103.
- (16) Wang, C.; Lu, H.; Wang, Z.; Xiu, P.; Zhou, B.; Zuo, G.; Wan, R.; Hu, J.; Fang, H. Stable Liquid Water Droplet on a Water Monolayer Formed at Room Temperature on Ionic Model Substrates. *Phys. Rev. Lett.* **2009**, *103*, 137801.

- (17) Xu, Z.; Gao, Y.; Wang, C.; Fang, H. Nanoscale Hydrophilicity on Metal Surfaces at Room Temperature: Coupling Lattice Constants and Crystal Faces. *J. Phys. Chem. C* **2015**, *119*, 20409–20415.
- (18) Limmer, D. T.; Willard, A. P.; Madden, P.; Chandler, D. Hydration of Metal Surfaces can be Dynamically Heterogeneous and Hydrophobic. *Proc. Natl. Acad. Sci. U.S.A.* **2013**, *110*, 4200–4205.
- (19) Kimmel, G. A.; Petrik, N. G.; Dohnalek, Z.; Kay, B. D. Crystalline Ice Growth on Pt(111): Observation of a Hydrophobic Water Monolayer. *Phys. Rev. Lett.* **2005**, 95, 166102.
- (20) Rafiee, J.; Mi, X.; Gullapalli, H.; Thomas, A. V.; Yavari, F.; Shi, Y.; Ajayan, P. M.; Koratkar, N. A. Wetting Transparency of Graphene. *Nat. Mater.* **2012**, *11*, 217–222.
- (21) Dai, X.; Sun, N.; Nielsen, S. O.; Stogin, B. B.; Wang, J.; Yang, S.; Wong, T.-S. Hydrophilic Directional Slippery Rough Surfaces for Water Harvesting. *Sci. Adv.* **2018**, *4*, No. eaaq0919.
- (22) Granick, S.; Bae, S. C. Chemistry: A Curious Antipathy for Water. Science 2008, 322, 1477-1478.
- (23) Poynor, A.; Hong, L.; Robinson, I. K.; Granick, S.; Zhang, Z.; Fenter, P. A. How Water Meets a Hydrophobic Surface. *Phys. Rev. Lett.* **2006**, *97*, 266101.
- (24) Guo, P.; Tu, Y.; Yang, J.; Wang, C.; Sheng, N.; Fang, H. Water-COOH Composite Structure with Enhanced Hydrophobicity Formed by Water Molecules Embedded into Carboxyl-Terminated Self-Assembled Monolayers. *Phys. Rev. Lett.* **2015**, *115*, 186101.
- (25) Giovambattista, N.; Debenedetti, P. J. Effect of Surface Polarity on Water Contact Angle and Interfacial Hydration Structure. *J. Phys. Chem. B* **2007**, *111*, 9581–9587.
- (26) Argyris, D.; Cole, A. Dynamic Behavior of Interfacial Water at the Silica Surface. *J. Phys. Chem. C* **2009**, *113*, 19591–19600.
- (27) Chialvo, A. A.; Vlcek, L.; Cummings, P. T. Surface Strain Effects on the Water-Graphene Interfacial and Confinement Behavior. *J. Phys. Chem. C* **2014**, *118*, 19701–19711.
- (28) Zhang, W.; Ye, C.; Hong, L. B.; Yang, Z. X.; Zhou, R. H. Molecular Structure and Dynamics of Water on Pristine and Strained Phosphorene: Wetting and Diffusion at Nanoscale. *Sci. Rep.* **2016**, *6*, 38327.
- (29) Heinz, H.; Vaia, R. A.; Farmer, B. L.; Naik, R. R. Accurate Simulation of Surfaces and Interfaces of Face-Centered Cubic Metals Using 12-6 and 9-6 Lennard-Jones Potentials. *J. Phys. Chem. C* **2008**, *112*, 17281–17290.
- (30) Fang, G.; Li, W.; Shen, X.; Perez-Aguilar, J. M.; Chong, Y.; Gao, X.; Chai, Z.; Chen, C.; Ge, C.; Zhou, R. Differential Pd-Nanocrystal Facets Demonstrate Distinct Antibacterial Activity against Gram-Positive and Gram-Negative Bacteria. *Nat. Commun.* **2018**, *9*. 129.
- (31) Heinz, H.; Farmer, B. L.; Pandey, R. B.; Slocik, J. M.; Patnaik, S. S.; Pachter, R.; Naik, R. R. Nature of Molecular Interactions of Peptides with Gold, Palladium, and Pd-Au Bimetal Surfaces in Aqueous Solution. *J. Am. Chem. Soc.* **2009**, *131*, 9704–9714.
- (32) Riccardi, L.; Gabrielli, L.; Sun, X.; De Biasi, F.; Rastrelli, F.; Mancin, F.; De Vivo, M. Nanoparticle-Based Receptors Mimic Protein-Ligand Recognition. *Chem* **2017**, *3*, 92–109.
- (33) Yuet, P. K.; Blankschtein, D. Molecular Dynamics Simulation Study of Water Surfaces: Comparison of Flexible Water Models. *J. Phys. Chem. B* **2010**, *114*, 13786–13795.
- (34) Toukan, K.; Rahman, A. Molecular-Dynamics Study of Atomic Motions in Water. *Phys. Rev. B: Condens. Matter Mater. Phys.* **1985**, 31, 2643–2648.
- (35) Driskill, J.; Vanzo, D.; Bratko, D.; Luzar, A. Wetting Transparency of Graphene in Water. J. Chem. Phys. 2014, 141, 18C517.
- (36) LAMMPS. http://lammps.sandia.gov (accessed November 26, 2019).
- (37) Hockney, R. W.; Eastwood, J. W. Computer Simulation Using Particles, 2nd ed.; IOP: Bristol, U.K., 1988.
- (38) Kim, J.-Y.; Greer, J. R. Tensile and Compressive Behavior of Gold and Molybdenum Single Crystals at the Nano-scale. *Acta Mater.* **2009**, *57*, 5245–5253.

- (39) Bachurin, D. V.; Gumbsch, P. Atomistic Simulation of the Deformation of Nanocrystalline Palladium: The Effect of Voids. *Modell. Simul. Mater. Sci. Eng.* **2014**, 22, 025011.
- (40) Phan, A.; Ho, T. A.; Cole, D. R.; Striolo, A. Molecular Structure and Dynamics in Thin Water Films at Metal Oxide Surfaces: Magnesium, Aluminum, and Silicon Oxide Surfaces. *J. Phys. Chem. C* **2012**, *116*, 15962–15973.
- (41) Tocci, G.; Joly, L.; Michaelides, A. Friction of Water on Graphene and Hexagonal Boron Nitride from Ab Initio Methods: Very Different Slippage Despite Very Similar Interface Structures. *Nano Lett.* **2014**, *14*, 6872–6877.
- (42) Ho, T. A.; Papavassiliou, D. V.; Lee, L. L.; Striolo, A. Liquid Water can Slip on a Hydrophilic Surface. *Proc. Natl. Acad. Sci. U.S.A.* **2011**, *108*, 16170–16175.
- (43) Zhou, R. Trp-Cage: Folding Free Energy Landscape in Explicit Water. Proc. Natl. Acad. Sci. U.S.A. 2003, 100, 13280–13285.